Surface Plasmon Resonance Effect of Ag Layer Inserted in a Highly Flexible Transparent IZTO/Ag/IZTO Multilayer Electrode for Flexible Organic Light Emitting Diodes

Ho-Kyun Park[1], Nam-Ho Jun[1], Kwang-Hyuk Choi[1], and Han-Ki Kim[1*]
[1]School of Advanced Materials and Systems Engineering, Kumoh National Institute of Technology (KIT), Gumi 730-701, Republic of Korea
TEL: +82-54-478-7746, e-mail: hkkim@kumoh.ac.kr

Keywords: **Transparent conducting oxide, Surface Plasmon Resonance, OLEDs.**

Abstract

We report on the Ag thickness effect on the electrical and optical properties of indium zinc tin oxide (IZTO)-Ag-IZTO multilayer electrode grown on a PET substrate and the surface plasmon effect of Ag layer on the optical properties of IZTO-Ag-IZTO electrode. Using an IZTO-Ag-IZTO multilayer with a total thickness below ~80 nm, we can obtain high-quality flexible electrode with very low sheet resistance, high transmittance, high work function and superior flexibility.

1. Introduction

Indium-tin-oxide (ITO) is the most commonly used electrode material in flat panel display (FPD) as it provides good electrical conductivity and high transparency in the visible region. Moreover, for FPD based on organic light-emitting diodes (OLEDs), ITO is the preferred anode material as it provides good energy-level alignment for the efficient injection of holes into the organic layers[1-3]. An alternative to a simple ITO film for transparent conductors is the use of dielectric–metal–dielectric (DMD) multilayers, also known as ITO–metal–ITO (IMI) when ITO is used instead of dielectric cladding layers. These structures are typically composed of a thin silver layer (~10–15 nm) sandwiched between two high dielectric constant layers (~30–50 nm). When designed properly, the high index of refraction contrast between Ag and the dielectric layers results in efficient plasmon coupling and visible transparency greater than 90% can be achieved.[4,5] However, the low work function of ITO (~4.7 eV) could result in imperfect work function alignment with hole injection layers or extraction layers in flexible OLEDs or OPVs. In addition, conventional amorphous ITO films grown on polymer substrate have several problems, such as high sheet resistance and low transmittance due to low sputtering temperature. Therefore, it is desirable to substitute amorphous ITO electrode with another TCO with low resistance, high transparency, superior flexibility, and a high work function.

In this work, we report on the properties of an indium-zinc-tin-oxide (IZTO)-Ag-IZTO multilayer electrode grown on polyethylene terephthalate (PET) substrate at room temperature and the surface plasmon resonance effect of the Ag layer on the optical properties of IZTO-Ag-IZTO electrode. Using an IZTO-Ag-IZTO multilayer with a total thickness below ~80 nm, we can obtain high-quality flexible electrode with very low sheet resistance, high transmittance, high work function and superior flexibility.

2. Experimental

Both top and bottom IZTO films with a thickness of 30 nm were deposited on a 200 μm thick PET substrate using rf (13.56 MHz) magnetron sputtering system at a constant Ar low rate of 20 sccm, working pressure of 3 mTorr and rf power of 120 W. After deposition of the bottom IZTO film, Ag layer was deposited onto the IZTO film by thermal evaporation at a constant deposition rate of 0.02 nm/s. Sheet resistance of the IZTO-Ag-IZTO anode was measured as a function of Ag thickness by means of a four-point probe measurement. The transmittance of the IZTO-Ag-IZTO multilayer was measured in the wavelength range of 200-800 nm using a UV/visible spectrometer. The surface morphology of the Ag layer on the bottom IZTO film was analyzed as a function of Ag thickness using field emission scanning electron microscope (FESEM). Finally, the flexibility of the IZTO-Ag-IZTO multilayer was analyzed using a laboratory made bending test system. The structural properties of IZTO-Ag-IZTO layer were analysis by XRD examination.

3. Results and discussion

Fig. 1 shows the sheet resistance, optical transmittance, and figure of merit (Φ_{TC}) of the IZTO-Ag-IZTO electrode on a PET substrate as a function of Ag thickness. Insertion of transparent Ag interlayer led to a significant reduction in the sheet resistance, with a rapid decrease in the sheet resistance for Ag layer thicker than 8 nm.

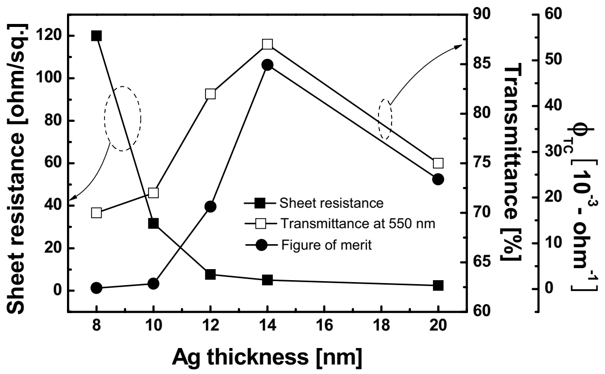

Fig. 1. Sheet resistance, transmittance at 550 nm wavelength, and figure of merit of and IZTO-Ag-IZTO multilayer electrode on PET substrate as a function of the Ag thickness.

An IZTO-Ag-IZTO multilayer with 14-nm-thick Ag layer, a sheet resistance of 4.99 Ω/sq. was seen. The transmittance of the IZTO-Ag-IZTO electrode at a 550 nm wavelength also depends on the thickness of Ag layer. At an Ag thickness of 8 nm, a fairly low transmittance of 66.8% at a 550 nm wavelength was seen due to the absorption of the aggregated Ag layer. However, IZTO-Ag-IZTO electrode with an Ag thickness of 14 nm showed the highest transmittance of 86% due to the surface plasmon resonance (SPR) of the Ag layer. It was reported that the high index of refraction contrast between Ag and the dielectric layer results in efficient plasmon coupling such that visible transparency greater than 90% can be achieved [1]. Therefore, the dramatically increased transmittance of an IZTO-Ag-IZTO electrode with an Ag thickness of 14 nm can be attributed to SPR of a properly designed Ag layer. However, further increase in Ag thickness resulted in a decrease in transmittance even though it had the lowest sheet resistance (2.4 Ω/ sq.). The figure of merit value (Φ_{TC}) value of the IZTO-Ag-IZTO multilayer also increases with increasing Ag thickness. The maximum Φ_{TC} value ($44 \times 10^{-3}\Omega^{-1}$) of the IZTO-Ag-IZTO multilayer was obtained at an Ag thickness of 14 nm (T: 0.86% and R_{sh}: 4.99 Ω/sq.). Further increases in the Ag thickness, however, lead to a decrease in Φ_{TC} value due to increased absorption by the Ag metal layer. Bender et al. showed that the maximum Φ_{TC} value of an ITO-Ag-ITO layer with 10 ~ 12-nm-thick metal layer on a glass substrate is 24.7 × $10^{-3}\Omega^{-1}$, which is lower than our results.[6] The higher Φ_{TC} value of the IZTO-Ag-IZTO multilayer on PET films indicates that IAI is a promising candidate to replace the ITO-Ag-ITO electrode in flexible OLEDs and OPVs.

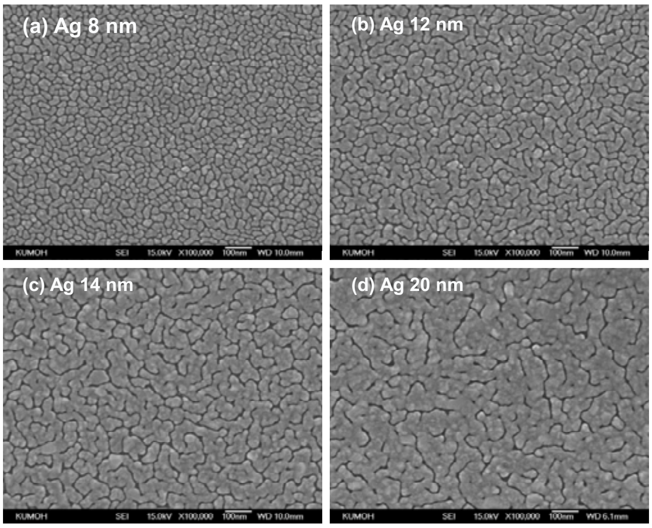

Fig. 2. Surface FESEM images of the Ag layer deposited on the bottom IZTO film with increasing Ag thickness of (a) 8 nm (b) 12 nm (c) 14 nm (d) 20nm

The Ag thickness dependence of the electrical and optical properties of an IZTO-Ag-IZTO electrode can be explained by the FESEM results in Fig. 2. The morphology and shape of the Ag layer clearly change with increasing Ag thickness. Fig. 2(a) and 2(b) show Ag layer with a thickness of less than 12 nm, in which a disconnected structure can be seen. This disconnected Ag layer corresponds to high sheet resistance and light absorption in IZTO-Ag-IZTO structure, as seen in Fig. 1. However, in the case of 14-nm-thick Ag film pictured in Fig. 2(c), the Ag layer was continuous. The low sheet resistance and high transmittance of the IZTO-Ag-IZTO multilayer with Ag thickness of 14 nm could be attributed to the fact that the Ag layer completely covered the bottom IZTO layer. FESEM results indicate that the effective SPR of the Ag layer occurred in the transition region from an aggregated Ag layer to a continuous Ag layer.

In the case of our IZTO-Ag-IZTO electrode, the optimized SPR can be found at a Ag thickness of 14 nm. Fahland *et al.* also reported that the critical thickness of the Ag layer for transition from distinct islands to a continuous film is predominantly between 10 and 20 nm [7].

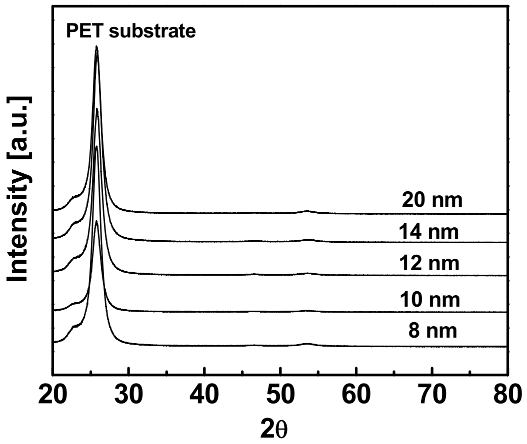

Fig. 3. XRD plot of IZTO-Ag-IZTO electrode as a function of Ag thickness

Figure 3 shows XRD plots of IZTO-Ag-IZTO electrode grown on a PET substrate as a function of Ag thickness. All XRD plows show only a PET substrate peak regardless of Ag thickness, indicative of amorphous IZTO and Ag structure. Due to low substrate temperature, both IZTO and Ag layer was deposited on a PET substrate as a type of amorphous structure.

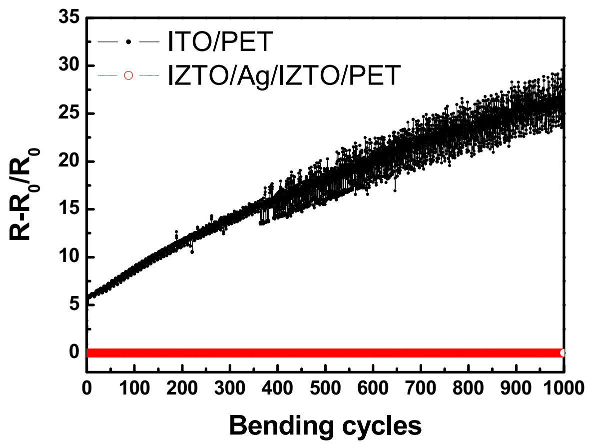

Fig. 4. Normalized resistance change after repeated bending as a function of the number of cycles for the reference ITO/PET, and IZTO-Ag-IZTO/PET.

To investigate the flexibility of the optimized IZTO-Ag-IZTO multilayer prepared on a PET substrate, a laboratory-made bending test system was employed.[8] For comparison, a reference ITO/PET sample was prepared using dc sputtering at room temperature. The change in resistance was expressed as ($R-R_0/R_0$), where R_0 is the initial resistance and R is the measured resistance after bending. Figure 4 shows changes in the resistance of the reference ITO/PET and IZTO-Ag-IZTO/PET sample. It was shown that the $R-R_0/R_0$ value of reference ITO/PET sample increased remarkably in initial bending cycles due to the generation and propagation of cracks. However, the IZTO-Ag-IZTO electrode exhibited a constant $R-R_0/R_0$ value, indicating constant resistance of the IZTO-Ag-IZTO electrode throughout the bending test. The robustness of the IZTO-Ag-IZTO multilayer is attributed to the existence of a ductile Ag metal layer between the IZTO layers. Lewis *et al.* reported that a ductile Ag layer between ITO layers provides effective electrical conductivity even after the ITO is beyond its failure strain (~0.8%) due to a higher failure strain of the bulklike Ag film (4% – 50%) [1].

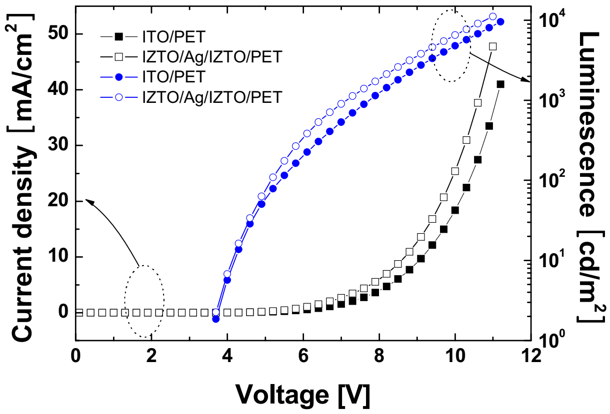

Fig. 4. Current density-voltage-luminance (J-V-L) characteristics of flexible OLEDs fabricated on IZTO-Ag-IZTO/PET and reference ITO/PET samples, respectively.

To compare the electrical and optical properties of flexible OLEDs fabricated on IZTO-Ag-IZTO/PET and a reference ITO/PET sample, we prepared flexible OLEDs on both the IZTO-Ag-IZTO anode and the reference ITO anode [10]. The fabrication process for producing a flexible OLED was described in detail in our previous reports.[8,9] The current density (J) of a flexible OLED fabricated on an IZTO-Ag-IZTO multilayer anode is higher than that of a flexible OLED fabricated on an ITO anode at the same voltage after a turn on of the flexible OLED. The L-V curve of the flexible OLEDs on the IZTO-Ag-IZTO multilayer also exhibits higher luminance than that of a flexible OLED on the a-ITO/PET sample as expected from the J-V curve. Due to a lower Ohmic loss and the higher work function of the IZTO layer in the IZTO-Ag-IZTO/PET sample than the ITO/PET sample, the flexible OLED on the IZTO-Ag-IZTO anode shows higher current density and luminance. The measured work function of the UV ozone-treated IZTO-Ag-IZTO electrode by photoelectron spectroscopy with a UV source is between 5.12 ± 0.02 eV. Therefore, the high performance of flexible OLEDs on an IZTO-Ag-IZTO multilayer anode can be attributed to the low sheet resistance of the IZTO-Ag-IZTO electrode and high transmittance caused by SPR of the Ag metal layer sandwiched between the two IZTO electrodes. Furthermore, the higher work function of the IZTO layer (~5.12 eV) compared to that of the reference ITO (4.7–4.9 eV) layer can lead to a lower barrier height between the IZTO electrode and the organic layer.

4. Summary

The IZTO-Ag-IZTO multilayer on a PET substrate had a low sheet resistance of 4.99 Ohm/square and high transmittance of 86% despite the fact that the IZTO layer was very thin (~30 nm). An Ag metal layer with a critical thickness of 14 nm sandwiched between two IZTO layers was shown to provide significantly improved sheet resistance and transmittance as well as mechanical robustness upon bending. Due to the SPR effect of the 14-nm-thick Ag layer, we can obtain IZTO-Ag-IZTO electrode with high transmittance as well as superior flexibility. This indicates that an IZTO-Ag-IZTO multilayer on polymer substrates is a promising flexible electrode scheme that can be used as a substitute for a conventional ITO anode or ITO-Ag-ITO on polymer substrates.

5. References

1. Jay Lewis, Sonia Grego, Babu Chalamala, Erik Vick, and Dorota temple, *Appl. Phys. Lett*., **85**, P3450 (2004).
2. F. Nuesch, E. W. Forsythe, Q. T. Le, Y. Gao, and L. J. Rothberg, *J. Appl. Phys*., **87**, 7973 (2000).
3. M. G. Mason, L. S. Hung, C. W. Tang, S. T. Lee, K. W. Wong, and M. Wang, *J. Appl. Phys*. **86**, 1688 (1999)
4. X. Liu, X. Cai, J. Qiao, J. Mao, and N. Jiang, *Thin Solid Films,* **441**, 200 (2003).
5. X. Liu, X. Cai, J. Mao, and C. Jin, *Appl. Surf. Sci*., **183**, 103 (2001).
6. M. Bender, W. Seelig, C. Dube, H. Fankenberger, B. Ocker, and J. Stollenwerk, *Thin Solid films* **326**, 67 (1998)
7. M. Fahland, P. Karsson, and C. Charton, *Thin solid films* **392**, 334 (2001)
8. J. -W. Kang, W. -I. Jeong, J. -J. Kim, J. -W. Kang, D. -G. Lee, *Electochem. Solid-state. Lett.*, **10** ,75 (2007).
9. J.-H. Bae, J.-M. Moon, J.-W. Kang, H.-D. Park, J.-J. Kim, W. J. Cho, and .-K. Kim, *J. Electrochem. Soc*. **154**, 81 (2007).
10. K.-H. Choi, H.-J. Nam, J.-A. Jeong, S.-W. Cho, H.-K. Kim, J.-W. Kang, D.-G. Kim, and W.-J. Cho, *Appl. Phys. Lett.* **92**, 2232302 (2008)